Poly-eugenol grafting from cellulose surface for robust antioxidation

Yiwei Li, Boya Yuan, Shibo Yu, Zhonghua Xia, Yoshiharu Nishiyama, Pan Chen, Wei Li, Minmin Liang

Graphical Abstract

Poly-eugenol grafting from cellulose surface for robust antioxidation

Yiwei Li,Boya Yuan,Shibo Yu,Zhonghua Xia,Yoshiharu Nishiyama,Pan Chen,Wei Li,Minmin Liang

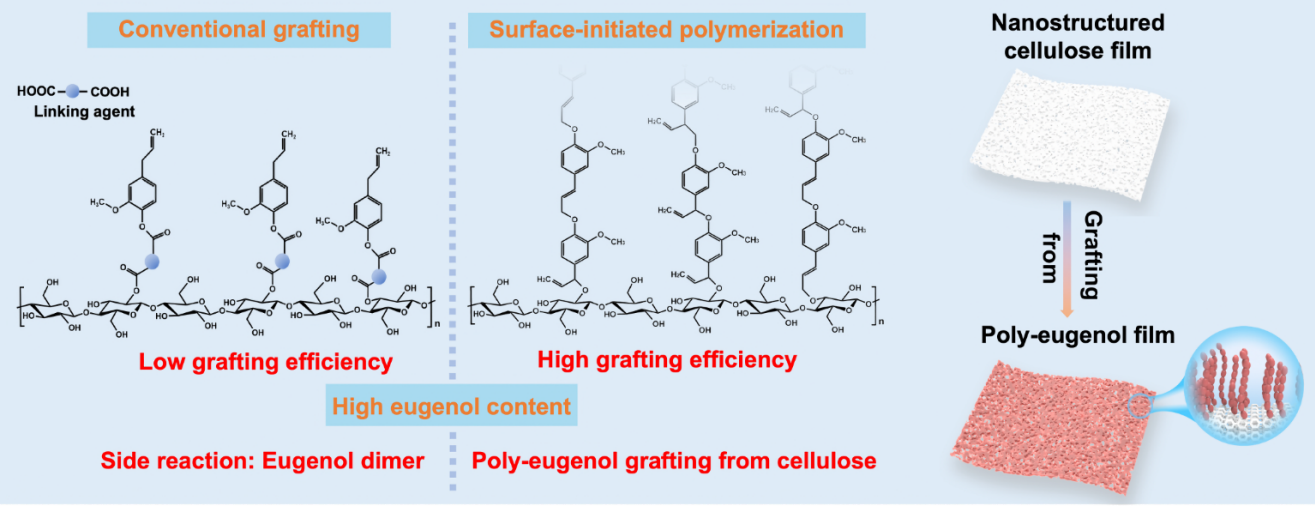

Poly-eugenol grafting from cellulose surface for robust antioxidation

Yiwei Li[a], Boya Yuan[a], Shibo Yu[a], Zhonghua Xia[a], Yoshiharu Nishiyama[b], Pan Chen[a], Wei Li[a,c,*] and Minmin Liang[a,*]

[a]School of Materials Science and Engineering Beijing Institute of Technology 100081 Beijing P.R. China
[b]Univ. Grenoble Alpes CNRS CERMAV 38000 Grenoble France
[c]Tangshan Research Institute Beijing Institute of Technology 063000 Tangshan P.R. China

ARTICLE INFO

Keywords:
Cellulose
Grafting from
Antioxidation
Reusability

ABSTRACT

This work not only eliminates the limitations and preserves the inherent advantages of eugenol but also imparts controllable hydrophobic and antioxidative properties to cellulose-based packaging. Eugenol, a prototypical natural phenolic compound, was immobilized by chemical linkage onto cellulose. A quantitative analysis based on Fourier-transform infrared spectroscopy (FTIR) and X-ray photoelectron spectroscopy (XPS) suggests a poly-eugenol structure on cellulose surface. Increasing the specific surface of cellulose by freeze-drying increased the reaction efficiency. The resulting material shows a robust antioxidant activity and tunable hydrophobility, making it a promising candidate for diverse applications.

1. Introduction

Antioxidative packaging is a crucial component in food and cosmetics industry, due to the ability of extending the shelf life, maintaining the quality of products and reducing the need for preservatives (Kanazawa, Sawa, Akaike and Maeda, 2002; Alamed, Chaiyasit, McClements and Decker, 2009; Kuai, Liu, Chiou, Avena-Bustillos, McHugh and Zhong, 2021). Eugenol, a simple phenolic compound, has earned substantial attention for its myriad of beneficial properties, including antioxidant, antimicrobial, analgesic, and anti-inflammatory activities (Pramod, Ansari and Ali, 2010; Ulanowska and Olas, 2021). However, its inherent volatility (Zhang, Lu, Wang, Shen, Hao, Li, J., Niu, Xiao, Chen and Zhang, 2021) and potential toxicity (Pramod et al., 2010; WHO, 2017) have hindered broader utilization. One way of eliminating limitations while preserving the inherent advantages of eugenol, centered on utilization of cellulose as an ideal substrate to address the aforementioned issues of eugenol.

Cellulose film is a potential packaging material with relatively high oxygen barrier properties in dry conditions but swells under high humidity, reducing this barrier property. The hydroxy groups on the surfaces are partly responsible for this swelling to provide potential covalent binding sites for the eugenol. There are few reports of grafting eugenol on cellulose. Muratore et al. (Muratore, Martini and Barbosa, 2018) used 1,2,3,4-butanetetracarboxylic acid (BTCA) as a linker to react on both phenolic group of eugenol and the hydroxy groups of cellulose. Although there is no quantification of grafted eugenol amount, the paper treated with BTCA and eugenol showed enhanced antioxidant and insecticide properties.

Since the phenolic hydroxy groups are associated with the antioxidant activity (Leopoldini, Marino, Russo and Toscano, 2004), preservation of both the phenolic hydroxy group and the double bond within the eugenol would be beneficial for the antioxidant properties. Zanarotti (Antonio, 1985) showed a process of coupling eugenol to the hydroxy group of methanol, conserving the double bonds and the phenol group. Although cellulose can be considered as a polyalcohol, its insolubility in the reaction medium leads at best to a heterogeneous reaction. In the study by Zanarotti, eugenol was reacted with excess methanol and the phenol groups were not participating in the reaction. However, in the heterogeneous reaction, the available hydroxy groups of cellulose can be limited, and the eugenol phenol might also participate to the reaction. In heterogeneous reactions, the accessible surface area is a critical factor influencing grafting efficiency, thereby enabling precise control of material properties. In this study, we modified the accessible surface area by modulating the drying conditions and quantified the immobilized eugenol to investigate its grafting behavior on the solid surface, and checked its anti-oxidant activities.

2. Experimental details

2.1. Materials

Cellulose, with a degree of polymerization (DP_w) of about 900, was purchased from Shanghai Yien Chemical Technology Co., Ltd. Urea (99%), lithium hydroxide hydrate (98%), p-toluene sulfonic acid (PTSA, 99%), and tetrahydrofuran (THF, ≥ 99.5%) were also obtained from Shanghai Yien Chemical Technology Co., Ltd. N,N-Dimethylformamide (DMF, ≥ 99.5%), dimethyl sulfoxide (DMSO, ≥ 99.0%), chloroform ($CHCl_3$, ≥ 99%), sulfuric acid (H_2SO_4, 95-98%), anhydrous methanol (≥ 99.5%), and n-butanol (≥ 99.5%) were provided by Shanghai Titan Technology Co., LTD. Eugenol (99%) and 1-diphenyl-2-trinitrophenylhydrazine (DPPH) were purchased from Sigma Aldrich. Carbon tetrachloride (CCl_4, ≥ 99.5%),

*Corresponding author
weili2021@bit.edu.cn (W. Li); mmliang@bit.edu.cn (M. Liang)
ORCID(s):

silver oxide (Ag_2O, $\geq$ 99%), and 2-thiobarbituric acid (2-TBA, 98%) were supplied by Shanghai Maclean Biochemical Technology Co., LTD. The 3-(4,5-dimethylthiazol-2-yl)-2,5-diphenyltetrazolium bromide (MTT) solution and formazan solvent from an MTT cell proliferation and cytotoxicity assay kit were obtained from Shanghai Beyotime Biotechnology Co., LTD. Hela cells were purchased from Nanjing Kebai Biotechnology Co., LTD. Dulbecco modified eagle medium (DMEM), fetal bovine serum (FBS), and penicillin-streptomycin solution were supplied by the Adamas-life brand of Shanghai Titan Technology Co., LTD.

2.2. Preparation of regenerated cellulose films

The LiOH/urea solution was prepared by mixing 9 g of $LiOH{\cdot}H_2O$, 12 g of urea, and 100 g of water. Then, 3.7 g of cellulose powder was mixed with the LiOH/urea solution and kept at -20 °C for 12 hours. The mixture was mechanically stirred for 20 minutes at room temperature and centrifuged at 8000 rpm and 4 °C for 5 minutes to remove bubbles, resulting in a transparent and viscous cellulose solution. The cellulose solution was poured onto a glass plate and spread evenly with a glass rod to obtain a gel sheet with a uniform thickness of about 2 mm. This sheet was then immersed in a 5 wt% H_2SO_4 solution for 20 minutes and rinsed with distilled water until the pH reached neutral. To dry the regenerated cellulose (RC) films, three different methods were used: air-drying in the ambient conditions, placing in a -80 °C freezer for 24 hours followed by lyophilization, and freezing in liquid nitrogen for about 20 minutes followed by lyophilization. The RC films dried using these methods were designated as a-RC, -80-RC, and n-RC, with respective thicknesses of approximately 0.09 mm, 0.15 mm, and 1.00 mm.

2.3. Grafting reaction between eugenol and regenerated cellulose films

The experimental protocol for the grafting reaction was modified from that reported by Antonio et al. (Antonio, 1985), and the detailed reasons for the modifications were specified in the *section "Exploration of surface initiated polymerization"* (Fig. S1a). Regenerated cellulose films (a-RC, -80-RC, and n-RC) of 300 mg (about 4 × 5 cm) were dried in an oven at 110 °C for 2 hours and transferred to a round-bottom flask containing 128 mL of dry DMSO. Separately, a mixture of eugenol (2 g), carbon tetrachloride (CCl_4, 320 mL), and silver oxide (Ag_2O, 12 g) was added into another round-bottom flask and reacted for 11 minutes in an oil bath at 65 °C. The resulting mixture was vacuum-filtered to remove solids, and the filtrate was poured into the flask containing DMSO solution and RC films. After the addition of 15.6 mL of a 5.8 mmol/L of p-toluenesulfonic acid (PTSA) solution in CCl_4/THF with a volume ratio of 5:2, the flask was placed in an oil bath at 90 °C. The reaction was stopped by taking out films that were successively washed with ethanol and then with distilled water. The films obtained from regenerated cellulose with different drying methods were named with a postfix corresponding to the reaction time: for example, films prepared from a-RC were designated as a-RCE0.5, a-RCE3, a-RCE7, a-RCE24, and a-RCE48, corresponding to the reaction time of 0.5, 3, 7, 24, and 48 hours, respectively.

2.4. Antioxidative activity measurement

5 mg of DPPH powder were dissolved in 100 mL of anhydrous methanol and stored in a dark environment at 4 °C. Next, 20 mg of the films were mixed with 4 mL of the DPPH solution and placed in the dark at 4 °C for 24 hours. The absorbance of the DPPH solution was measured at 515 nm using a Shimadzu UV-2600 spectrometer. The antioxidant activity of the films was expressed as the DPPH radical scavenging activity (DPPH-RSA, %) using the following equation.

$$DPPH - RSA = \frac{(A_{control} - A_{sample})}{A_{control}} \times 100\% \quad (1)$$

where $A_{control}$ and A_{sample} were the absorbance of the pure DPPH solution and the mixture of DPPH solution and the films, respectively.

2.5. Antioxidation stability via rinsing

The stability of the modified films was investigated by evaluating their antioxidation properties after rinsing with a range of organic solvents or through multiple rinsing cycles. Four organic solvents, specifically THF, $CHCl_3$, acetone, and DMF were utilized to wash the n-RCE0.5 films, each subjected to one rinsing cycle. More specifically, a single rinsing cycle comprised the immersion of approximately 25 mg of the n-RCE0.5 films in 10 mL of each solvent for one hour, succeeded by a washing procedure with water. To evaluate the impact of repeated rinsing cycles, the n-RCE0.5 films underwent rinsing with acetone for one and ten cycles, respectively. Following the completion of the rinsing process, the films were frozen in liquid nitrogen and subsequently lyophilized. The antioxidative activity of the obtained films was measured by employing the DPPH radical scavenging assay, as delineated in the *section "Antioxidative activity measurement"*.

2.6. Cytotoxicity assay

The cytotoxicity of n-RC and n-RCE0.5 films was evaluated using the MTT method. Round discs with a diameter of 6 mm were cut from the films and sterilized at 121 °C for 15 minutes. To prepare the culture medium, DMEM was supplemented with 10% sterile fetal bovine serum (FBS) and 1% sterile penicillin-streptomycin solution. Human cervical cancer (Hela) cells were seeded in a 96-well plate, with each well containing 100 μL DMEM. The cells were then incubated in a 5% CO_2 incubator at 37 °C for 24 hours. Next, the DMEM medium was replaced with fresh medium, and the sterile n-RC and n-RCE0.5 films were added to the wells. After incubating the cells for 24 hours, 10 μL of MTT solution (5 mg/mL) was added to each well, and the plate was incubated at 37°C for 4 hours in the absence of light. Formazan solvent (100 μL) was then added to each

well to dissolve the purple crystals formed from MTT. The films were removed from the wells, and the absorbance of the mixed solution at 570 nm was measured using a multimode plate reader (VICTOR Nivo, PerkinElmer, China). The wells containing only DMEM medium without Hela cells and films were served as the blank, while those containing DMEM medium and Hela cells without any film were considered as the control. Statistical analysis was performed, including the calculation of means and hypothesis testing using p-values, based on triplicate measurements for each sample. The relative growth rate (RGR, %) of cells was calculated using the following formula.

$$RGR = \frac{(A_{sample} - A_{blank})}{(A_{control} - A_{blank})} \quad (2)$$

where A_{sample}, A_{blank} and $A_{control}$ were the absorbance of the samples, the blank and the control, respectively.

2.7. Fat meat oxidation essay during preservation

Fresh pork fat meat, purchased from a local supermarket in Beijing, was cut into 200 mg pieces with equal weight and packaged in n-RC films and n-RCE0.5 films. A control sample was also included, consisting of fat meat without any packaging. All samples were preserved at a room temperature of approximately 22 °C for 1 and 6 days. The oxidation degree of the fat meat was detected using the method specified in China National Standard GB_T 35252-2017(General Administration of Quality Supervision, Inspection and Quarantine of the People's Republic of China, 2017). Malondialdehyde (MDA), the secondary oxidation product of the fat meat, was reacted with a 2-TBA solution. The resulting mixture changed from light yellow to pink and exhibited the maximum absorption peak at 530 nm. The TBA value reflects the degree of oxidation in the fat meat.

2.8. Characterization

Nitrogen adsorption Nitrogen adsorption isotherm was measured using a V-Sorb 2800P specific surface area analyzer from Golden Spectrum Technology Co., LTD., China. The films were degassed at 80 °C for 10 h and the specific surface area of the films was calculated using Brunauer - Emmett - Teller (BET) theory(Brunauer, Emmett and Teller, 1938).

Infrared spectroscopy Attenuated total reflection Fourier-transform infrared (ATR-FTIR) spectra were collected and presented with ATR correction using a Thermo Scientific Nicolet iS50 Fourier Transform Infrared spectrometer. The Python script-1 and scrip-2 for analyzing the infrared data are shown in the Supplementary data.

X-ray photoelectron spectroscopy (XPS) analysis was obtained on a PHI quantera SXM X-ray photoelectron spectrometer from the ULVAC-PHI in Japan, equipped with a monochromatic Al Kα X-ray source (hν = 1486.7 eV). The photoelectron takeoff angle relative to the sample surface was 45°. The XPSPEAK41 software was used for background subtraction (Shirley-type) and fitting.

Scanning electron microscopy (SEM) A Regulus 8230 cold field emission scanning electron microscope of Hitachi High-Tech of Japan was used. The samples were gold sputter-coated and the topography was obtained at an accelerating voltage of 3 kV.

Contact angles of the films was investigated using a Dataphysics OCA-20 contact angle analyzer from Dataphysics, Germany. A volume of 50 μL of distilled water was dripped onto a rectangular film strip, and the resulting angle at which the water droplets came into contact with the film was meticulously recorded and quantified.

Thermogravimetric (TG) curves and derivative thermogravimetry (DTG) curves were obtained using a thermogravimetric analyzer (STA 449 F5) of NETZSCH, Germany from 50 °C to 600 °C at a heating rate of 10 °C/min.

X-ray diffraction (XRD) analysis was performed using a Bruker D8 diffractometer from the Bruker company in Germany with the Cu Kα (λ = 0.154 nm) radiation and the geometry of Bragg-Brentano.

3. Results and discussion

3.1. Overview of surface initiated polymerization

The schematic illustration for the poly-eugenol grafting from nanostructured cellulose films is depicted in Fig. 1. Cellulose film with high specific surface area and porous morphology is fabricated from native cellulose powder. The nanostructured cellulose film exhibits low solubility in common solvents, which results in its insolubility within the reaction mixture when interacting with eugenol. Consequently, this leads to a heterogeneous reaction. Due to such characteristics, not all hydroxy groups present in the cellulose films are readily accessible for grafting reactions with eugenol molecules. Only those hydroxy groups situated on the surface are available for this reaction. Meanwhile, eugenol molecules firstly undergo complete conversion to the reaction intermediate after activation (Fig. S1b). There are two possible chemical structures (I and II) of the initial product (Antonio, 1985). The persistent presence of hydroxy groups in the initial product can continuously react with the reaction intermediates, resulting in the formation of poly-eugenol structures.

Fig. 2a displays the surface morphology of both regenerated and modified cellulose films, along with digital photographs, and the contact angles images of the respective films in the insets. When air-dried, the a-RC films are non-porous, highly transparent and colorless, but fibrillar impression can be observed on the SEM micrographs. As the reaction time increased, the fibrous morphology gradually disappear, resulting in granulated films that are less transparent and have a light brown color. For regenerated cellulose films that undergo freeze at -80 °C before lyophilization, partially porous surfaces are observed, resulting in opaque and white -80-RC films. After chemical modification, the porous structure is maintained, while the pore skeleton is coated

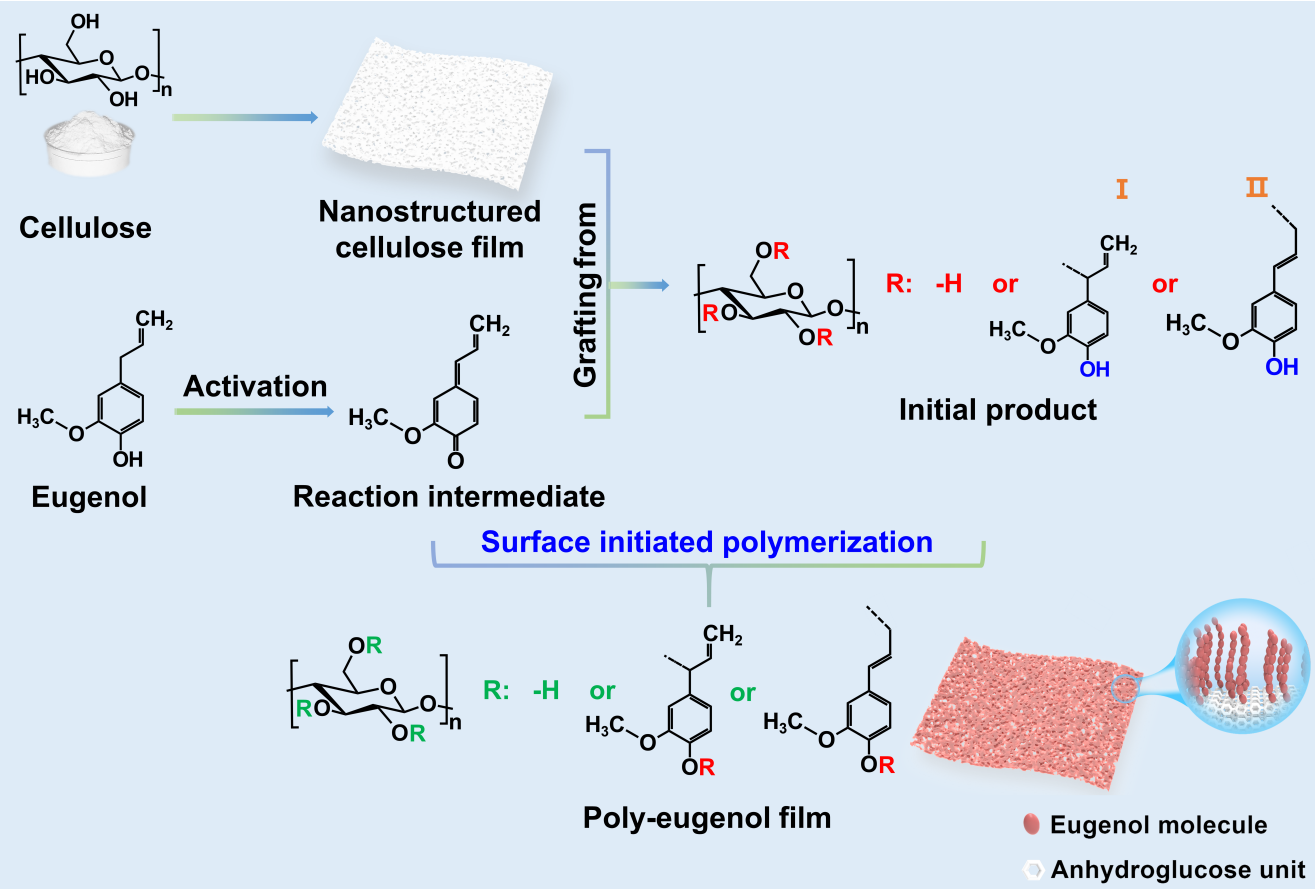

Fig. 1: The schematic illustrations for the surface-initiated polymerization of eugenol.

with a gel-like layer. Moreover, granule-like morphology is not observed even with a reaction time of 48 hours. The modified films become progressively less transparent, and their colors change to dark brown with increasing reaction time. In contrast, when regenerated cellulose films are lyophilized after liquid nitrogen freeze, highly porous and completely opaque n-RC films are produced. After modification, the films retain their high porosity and opacity, but the color changes from white to brown with increasing reaction time. Furthermore, the colors of modified films remain nearly constant after washing with ethanol. The contact angles of a-RC, -80-RC, and n-RC films are 40°, 9°, and 4°, respectively. This indicates that a porous structure, with greater exposure of hydroxyl groups, enhances wettability. After eugenol grafting, the contact angles of cellulose films increase with the reaction time. Notably, the -80-RCE48 film exhibites the highest contact angle of 100°. The enhancement of hydrophobicity in the modified films occurs because the hydrophilic hydroxy groups in cellulose molecules were replaced by hydrophobic eugenol moieties during grafting. Fig. S2 provides the changes in surface morphology and hydrophobicity of the modified films under reaction time of 3h, 7h, and 24h. XRD patterns of the modified films retained the characteristic cellulose II structure, but the crystallinity of the modified films varies depending on the drying methods and reaction time (Fig.S3). In summary, the drying method and reaction time significantly influence the the surface morphology, transparency, color and surface wettability of the cellulose films.

Fig. 2b shows the infrared spectra of eugenol, cellulose and poly-eugenol film. In the infrared spectrum of eugenol, broad bands at around 3600 - 3300 cm^{-1} are assigned to the stretching vibration of hydroxyl groups (Higgins, Stewart and Harrington, 1961). The characteristic peak at 1515 cm^{-1} originates from C=C stretching (Yang and Song, 2005; Kayaci, Ertas and Uyar, 2013), while a series of absorption bands in the 1250-799 cm^{-1} range are caused by the in-plane bending vibration of C-H in the benzene rings (Smith, 2016). In the spectrum of cellulose, the stretching of the hydroxyl groups results in a strong and wide characteristic peak at about 3300 cm^{-1}, while the strong absorbance at 1060 cm^{-1} is ascribed to the stretching vibration of C-O-C (Higgins et al., 1961). After the grafting reaction, the poly-eugenol film retains the main characteristic peaks of cellulose, while new peaks appear at 1515 cm^{-1} and 799 cm^{-1}, corresponding to the C=C and =C-H from the eugenol moieties, respectively. High resolution XPS spectrum of C_1s fitting curves for the poly-eugenol film is presented in Fig. 2c. In the C_1s spectrum of the regenerated cellulose film, a single peak corresponding to the sp^3 hybridized carbon of cellulose was observed (Fig. S4a). Conversely, in the poly-eugenol film, two distinct signals emerged at approximately

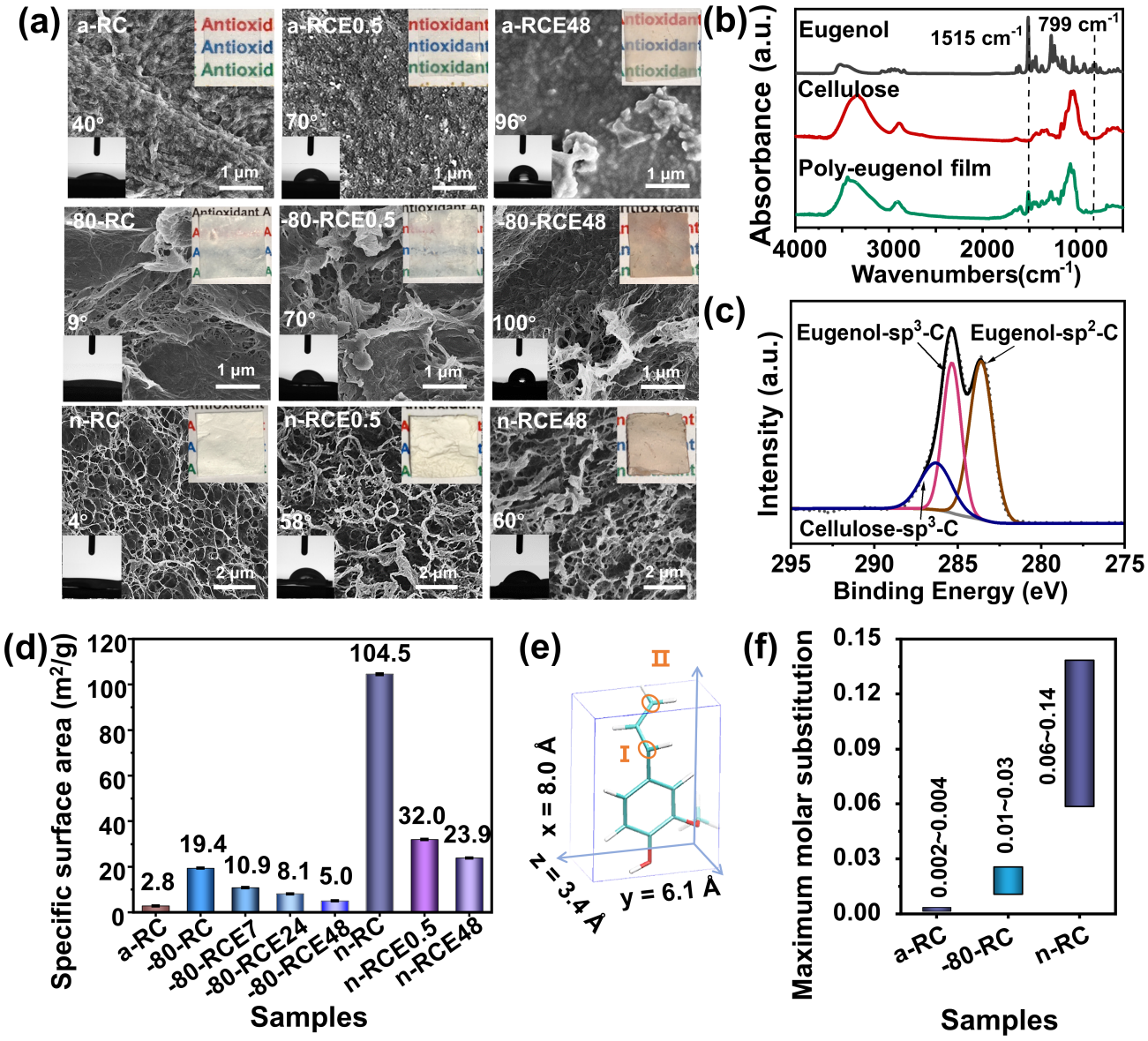

Fig. 2: (a) SEM images, the inserted digital photos (right top) and contact angle images (left bottom) of the regenerated cellulose films and the modified films. (b) Infrared spectra of eugenol, cellulose and poly-eugenol film. (c) High resolution XPS spectrum of C_1s fitting curves for the poly-eugenol film. (d) Specific surface areas of the regenerated cellulose films and the modified films. (e) Size of an eugenol molecule. (f) Estimated maximum molar substitution ranges of the a-RC, -80-RC and n-RC films.

285 eV and 286 eV, attributed to the sp^3 hybridized carbon and sp^2 hybridized carbon of eugenol moieties, respectively. As the reaction time increases, the atomic ratio of eugenol moieties increases, as shown in Fig. S4. The ATR-FTIR results and XPS spectra confirmed that eugenol was successfully introduced into the poly-eugenol film.

The specific surface areas of the RC films and their corresponding modified films are shown in Fig. 2d. The specific surface areas of a-RC and -80-RC films are determined to be 2.8 m^2/g and 19.4 m^2/g, respectively. The n-RC film has the largest specific surface areas of 104.5 m^2/g. Under the assumption that each square nanometer of cellulose can accommodate two hydroxy groups, these specific surface areas indicate the presence of 5.6×10^{18}, 3.9×10^{19}, and 2.1×10^{20} hydroxy groups per gram available for eugenol grafting in the a-RC, -80-RC, and n-RC films, respectively. For heterogeneous reaction, steric hindrance is one of the significant factors influencing the molar substitution of the modified films. Consequently, under the circumstance of single grafting, the theoretical maximum molar substitution of these modified films can be deduced by taking into account the specific surface area of the original cellulose films. The size of an eugenol molecule shown in the Fig. 2e was calculated from the molecule structure of eugenol constructed by using the GaussView software. The calculation for the maximum amount of eugenol molecules

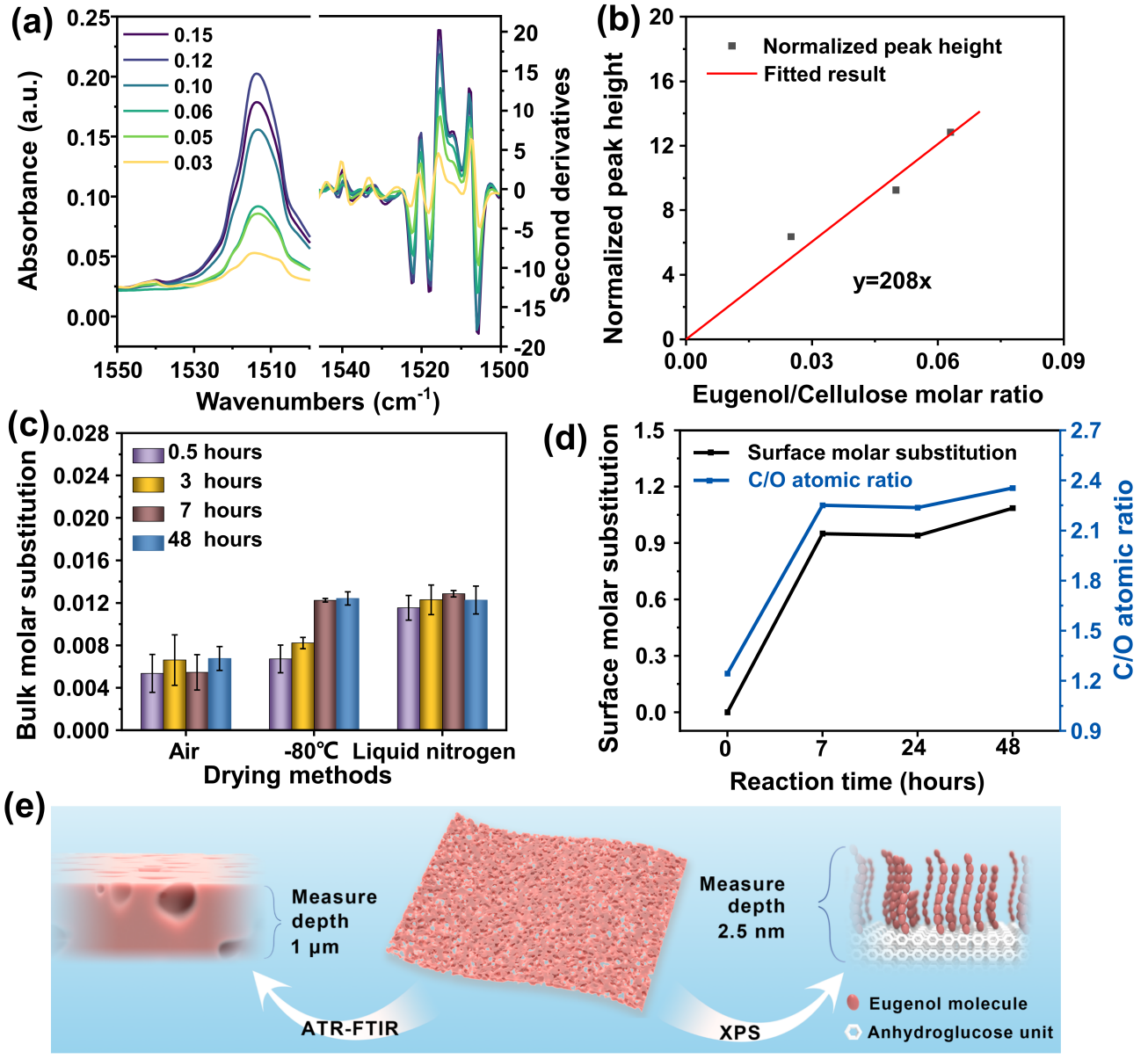

Fig. 3: Mechanistic studies of surface initiated polymerization. (a) The original infrared spectra and normalized second derivative infrared spectra of cellulose mixing with different amount of eugenol (molar ratio, 0.15, 0.12, 0.10, 0.06, 0.05, 0.03). (b) The peak height ratio of C=C at about 1515 cm^{-1} to that of C-O-C at about 1060 cm^{-1} in the infrared spectra. (c) The bulk molar substitution of the modified films estimated from ATR-FTIR spectra. (d) The C/O atomic ratio and surface molar substitution of the modified films with -80-RC and eugenol at reaction time 0 hours, 7 hours, 24 hours and 48 hours from XPS analysis. (e) The schematics of the measurement depths for ATR-FTIR and XPS analyses.

binding to one gram of cellulose utilizes the surface areas of one gram of RC films, divided by the area of either the yz or xy plane of an eugenol molecule. The resultant maximum molar substitution ranges are estimated and presented in Fig. 2f, signifying that the maximum molar substitution value for the modified films should not exceed 0.14. This estimation excludes considerations of intermolecular repulsion, wherein the actual molar substitution values might be even smaller than those illustrated in Fig. 2f.

3.2. Mechanistic studies of surface initiated polymerization

ATR-FTIR and XPS for quantitative analysis (Cichosz, Masek and Dems-Rudnicka, 2022; Ishimaru, Hata, Bronsveld, Meier and Imamura, 2007) are further employed to calculate the molar substitution on the surface of the modified films. To estimate the molar substitution of the modified films using ATR-FTIR spectra, it is essential to establish the correlation between the molar substitution value and the normalized FTIR peak height of the eugenol moiety. For this purpose, various combinations of mercerized cellulose

(100 mg, 50 mg, 40 mg, 25 mg, 20 mg, and 16 mg) were ground with 2.5 mg of eugenol using a mortar, resulting in eugenol/cellulose molar ratios of 0.03, 0.05, 0.06, 0.10, 0.12 and 0.15, respectively. The second derivative infrared spectra (Guerra-López, Güida and Della Védova, 2010) were used to avoid the influence from neighboring peaks, and then normalized with the peak at 1060 cm^{-1} (C-O-C strentching vibration from cellulose), as shown in the Fig. 3a. The relationship between the normalized peak height and the eugenol/cellulose ratio is depicted in Fig. 3b, exhibiting a well-fitted linear curve initially, but deviation occur when the eugenol/cellulose ratio exceeds 0.06. The discrepancy is primarily because when eugenol/cellulose ratio is high, eugenol is squeezed out from the sample during the ATR-FTIR measurement. Hence, eugenol/cellulose ratios exceeding 0.06 are not considered when calculating the fitting function.

The infrared spectra of the modified films are shown in Fig. S5, and the normalized peak height of the modified films summerized in Table S1. Based on the fitting function in Fig. 3b, the molar substitution values of the modified films are estimated and presented in the Fig. 3c. For the modified films prepared with air-dried cellulose films, the molar substitution values exhibit a higher degree of variability owing to the inherent heterogeneity of the substrate. For cellulose films that are frozen at -80 °C and subsequently lyophilized, the molar substitution values of the modified films increase with longer reaction time. When cellulose films are lyophilized after liquid nitrogen freeze, the molar substitution values of the modified films remain nearly constant at around 0.012, regardless of the reaction time.

The C/O atomic ratios, derived from the XPS spectra (Fig. S4) of the modified films under reaction time of 0 hours, 7 hours, 24 hours and 48 hours, are displayed in the Fig. 3a. Based on the C/O atomic ratios, the molar substitution values of the -80-RCE7, -80-RCE24 and -80-RCE48 films are calculated as 0.95, 0.94 and 1.09, respectively. Evidently, there exists a substantial difference between the molar substitution values estimated from ATR-FTIR (Fig. 3c) and XPS measurements (Fig. 3d). This difference is mainly due to the different measure depths between ATR-FTIR and XPS measurements. Considering the attenuation of the X-ray signal with increasing depth, the measure depth of the XPS analysis is approximately 2.5 nm (Wallart, Henry de Villeneuve and Allongue, 2005), whereas that of infrared spectroscopy is about 1 μm, as depicted in Fig. 3e. Considering the significant difference between the calculated molar substitution values from ATR-FTIR and XPS analysis, the proportion of eugenol within the XPS measure depth of the sample is substantially higher than that in the ATR-FTIR measure depth of the same sample. It is reasonable to hypothesize on the surface of cellulose, the hydroxy groups initiate polymerization of eugenol. This process results in the formation of a brush-like poly-eugenol structure.

3.3. Material properties

Fig. 4a illustrates the DPPH-RSA of the regenerated cellulose films and the eugenol grafted films. As demonstrated in Fig. 4a, the DPPH-RSA values of the a-RC, -80-RC, and n-RC films were only 1.0%, 3.0%, and 2.6%, respectively, indicating extremely low antioxidant activity in all of the unmodified cellulose films. However, the antioxidant activity of the eugenol grafted films significantly increased after the grafting reaction. For the air-dried films, the DPPH-RSA of the modified films gradually improved with an increase of the reaction time. The a-RCE48 film, with a reaction time of 48 hours, had a DPPH-RSA value of 47%, indicating a substantial increase in antioxidant activity. The films frozen at -80 °C and lyophilized required only 0.5 hours of the reaction time to achieve 77% of the DPPH-RSA value. The DPPH-RSA value of the -80-RCE7 film increased to 93% with an increase in reaction time, but a slight drop in the DPPH-RSA was observed at 24 and 48 hours. The n-RCE0.5 film, even with a reaction time of 0.5 hours, exhibited a DPPH-RSA value of 95%, and the DPPH-RSA value remained stable at around 95% at longer reaction time. The n-RCE0.5 film exhibits the highest reaction efficiency among the modified films (Fig.S6). Among the three different drying methods, lyophilization with liquid nitrogen freeze resulted in cellulose films with the largest specific surface area and most porous structure, as shown in the SEM images. This nano structure and higher specific surface area exposed more hydroxy groups of cellulose to be grafted with eugenol, thereby contributing to the higher antioxidant activity of the modified films. In summary, longer reaction time and larger specific surface area of the cellulose films enhance the antioxidant activity of the modified films.

Fig. 4b presents the thiobarbituric acid reactive substances (TBA) values for fat meat samples enclosed in n-RC and n-RCE0.5 films over a preservation period of 1 to 6 days. Initially, at day 1, the TBA values of the fat meat samples encased in the two different films were comparable, due to the low degree of lipid oxidation. After a preservation of 6 days, the unencapsulated fat meat manifested the highest TBA value, surpassing that of the fat meat wrapped in the n-RC films by approximately 1.7 fold. The fat meat packaged in the n-RCE0.5 films showed the most significant reduction in TBA values after the 6-day period, likely a consequence of the enhanced antioxidant property by the eugenol grafting.

To test the reusability of the modified films, the n-RCE0.5 films were washed with different organic solvents once or ten times. Fig. 4c displays the DPPH radical scavenging activities (DPPH-RSA) of the n-RCE0.5 films after being washed with THF, $CHCl_3$ and DMF for one time, and with acetone for one and ten times. The DPPH-RSA values of the n-RCE0.5 films washed with these solvents were all maintained at around 94%. It indicated the remarkable reusability and stability of the modified films in commonly used organic solvents. Fig. S7 confirms the critical role of Ag_2O in converting eugenol to the reaction intermediate, which is essential for forming covalent bonds between cellulose and eugenol. Without this transformation, eugenol

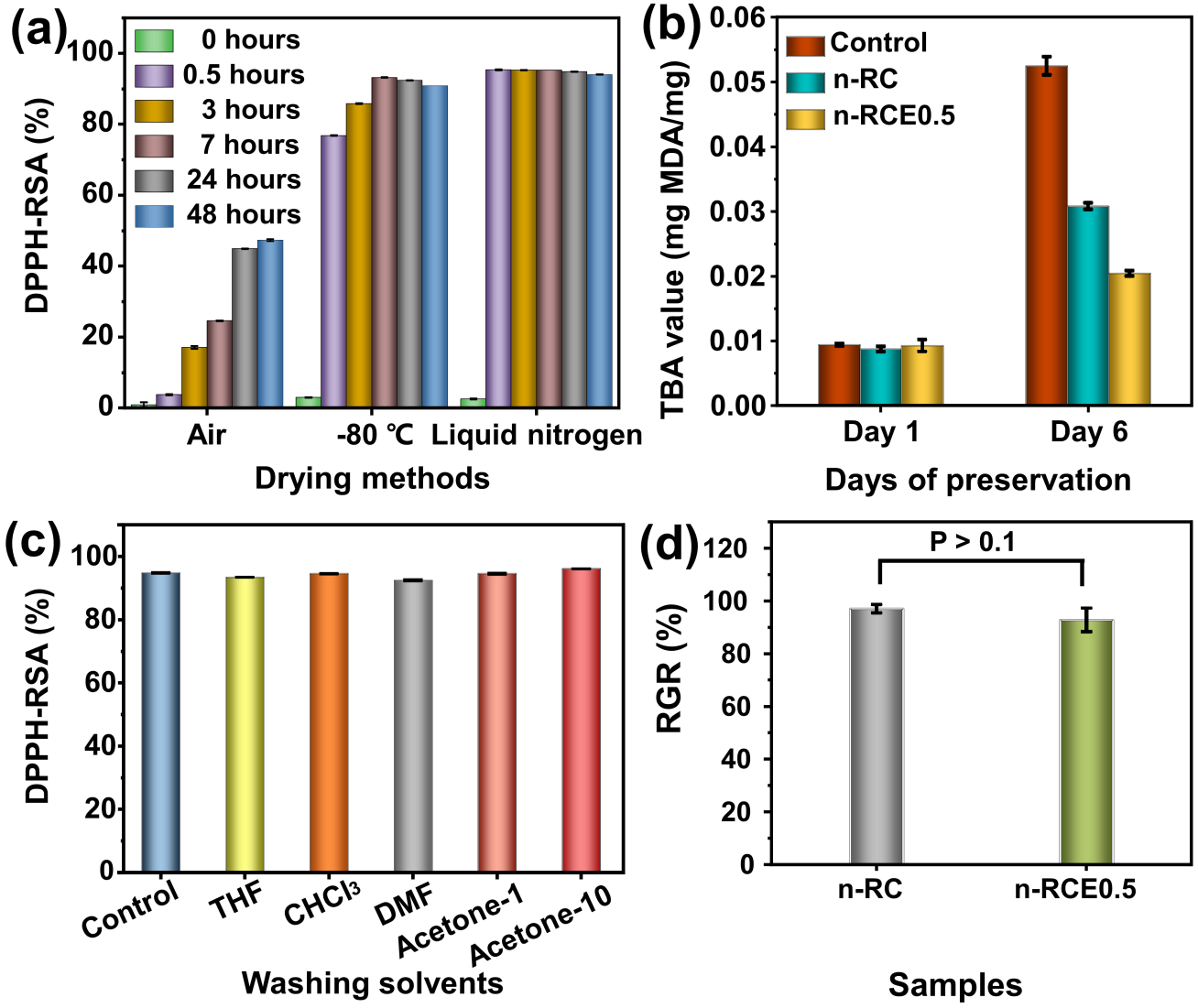

Fig. 4: (a) The (DPPH-RSA) of the modified films with the reaction time of 0.5 hours, 3 hours, 7 hours, 24 hours and 48 hours, and the drying methods of the cellulose films included air-drying (Air), -80 °C freeze and lyophilization (-80 °C), liquid nitrogen freeze and lyophilization (Liquid nitrogen). (b) The TBA values of the fat meat unpackaged (Control) and packaged in the n-RC and n-RCE0.5 films after preservation for 1 and 6 days. (c) The (DPPH-RSA) of the n-RCE0.5 films washed without solvent (Control) and with different solvents (THF, $CHCl_3$, DMF and Acetone-1) for one time and with acetone for ten times (Acetone-10). (d) The relative growth rates (RGR) of cells incubated with the n-RC and the n-RCE0.5 films.

is easily washed out due to the lack of covalent bonding. This explains the high reusability and stability of the poly-eugenol films against washing with organic solvents. In addition, the modified films exhibit increased thermal stability than cellulose films as shown in Fig. S8. Fig. 4d illustrates the relative growth rates (RGR) of HeLa cells cultured in the presence of n-RC and n-RCE0.5 films. The RGR for cells incubated with n-RC and n-RCE0.5 films were recorded at 97% and 93%, respectively. The statistical analysis shows that a p-value greater than 0.1 indicates no significant difference between the means of the two samples. This demonstrates that both n-RC and n-RCE0.5 films have minimal impact on cellular proliferation, confirming their high biocompatibility. Consequently, the poly-eugenol films are safe for direct food contact and hold promise for effective food preservation, preventing oxidative degradation during storage.

4. Conclusion

Eugenol molecules could be successfully grafted on cellulose as attested by its resistance to washing in diverse solvents, in contrast to the control without chemical reaction. The specific surface areas of the cellulose plays an important role as the freeze-drying at low temperature, with high surface area, the modified films achieved a DPPH-RSA value of 95% in just half an hour of reaction. The molar substitution values, derived from ATR-FTIR and XPS analyses, suggested the surface initiated polymerization. This approach

has potential applications in diverse fields including nanomaterials science, food preservation, pharmaceuticals, and environmental technology.

5. CRediT authorship contribution statement

Yiwei Li: Investigation, data analysis, original draft. Boya Yuan: Investigation. Zhonghua Xia & Pan Chen: Resources and review. Yoshiharu Nishiyama: Supervision and review. Wei Li: Project administrator, investigation, supervision, original draft and review. Minmin Liang: Project administrator, resources and review.

6. Declaration of competing interest

There are no conflicts of interest to declare.

7. Data availability

Data will be made available on request.

8. Acknowledgement

This work was supported by Beijing Institute of Technology Research Fund Program For Young Scholars (XSQD-202108010) and Natural Science Foundation of Hebei Province (B2023105020). We thank Experimental Center of Advanced Materials, Beijing Institute of Technology for characterization.

9. Appendix A. Supplementary data

Supplementary data to this article can be found online.

References

Alamed, J., Chaiyasit, W., McClements, D.J., Decker, E.A., 2009. Relationships between free radical scavenging and antioxidant activity in foods. Journal of Agricultural and Food Chemistry 7, 2969–2976.

Antonio, Z., 1985. Synthesis and reactivity of vinyl quinone methides. Journal of Organic Chemistry 50, 941–945.

Brunauer, S., Emmett, P.H., Teller, E., 1938. Adsorption of gases in multimolecular layers. Journal of the American Chemical Society 60, 309–319.

Cichosz, S., Masek, A., Dems-Rudnicka, K., 2022. Original study on mathematical models for analysis of cellulose water content from absorbance/wavenumber shifts in atr ft-ir spectrum. Scientific Reports 12, 19739.

General Administration of Quality Supervision, Inspection and Quarantine of the People's Republic of China, 2017. Determination of 2-thiobarbituric acid value in animal and vegetable fats and oils: Direct method. National Standard GB/T 35252-2017. Standardization Administration of China. Beijing, China.

Guerra-López, J., Güida, J., Della Védova, C., 2010. Infrared and raman studies on renal stones: the use of second derivative infrared spectra. Urological Research 38, 383–390.

Higgins, H., Stewart, C., Harrington, K., 1961. Infrared spectra of cellulose and related polysaccharides. Journal of polymer science 51, 59–84.

Ishimaru, K., Hata, T., Bronsveld, P., Meier, D., Imamura, Y., 2007. Spectroscopic analysis of carbonization behavior of wood, cellulose and lignin. Journal of materials science 42, 122–129.

Kanazawa, A., Sawa, T., Akaike, T., Maeda, H., 2002. Dietary lipid peroxidation products and dna damage in colon carcinogenesis. European Journal of Lipid Science and Technology 104, 439–447.

Kayaci, F., Ertas, Y., Uyar, T., 2013. Enhanced thermal stability of eugenol by cyclodextrin inclusion complex encapsulated in electrospun polymeric nanofibers. Journal of Agricultural and Food Chemistry 61, 8156–8165.

Kuai, L., Liu, F., Chiou, B.S., Avena-Bustillos, R.J., McHugh, T.H., Zhong, F., 2021. Controlled release of antioxidants from active food packaging: A review. Food Hydrocolloids 120, 106992.

Leopoldini, M., Marino, T., Russo, N., Toscano, M., 2004. Antioxidant properties of phenolic compounds: H-atom versus electron transfer mechanism. Journal of Physical Chemistry A 108, 4916–4922.

Muratore, F., Martini, R.E., Barbosa, S.E., 2018. Bioactive paper by eugenol grafting onto cellulose. effect of reaction variables. Food Packaging and Shelf Life 15, 159–168.

Pramod, K., Ansari, S.H., Ali, J., 2010. Eugenol: a natural compound with versatile pharmacological actions. Natural product communications 5, 1999–2006.

Smith, B., 2016. Group wavenumbers and an introduction to the spectroscopy of benzene rings .

Ulanowska, M., Olas, B., 2021. Biological properties and prospects for the application of eugenol—a review. International Journal of Molecular Sciences 22, 3671.

Wallart, X., Henry de Villeneuve, C., Allongue, P., 2005. Truly quantitative xps characterization of organic monolayers on silicon: Study of alkyl and alkoxy monolayers on h-si(111). Journal of the American Chemical Society 127, 7871–7878.

WHO, 2017. World health organization. iarcmonographs on the identification of carcinnogenic hazards to humans,agents classified by the iarc monographs. https://monographs.iarc.who.int/agents-classified-by-the-iarc/.

Yang, Y., Song, L., 2005. Study on the inclusion compounds of eugenol with alpha-, beta-, gama- and heptakis (2,6-di-o-methyl)-beta-cyclodextrins. Journal of Inclusion Phenomena and Macrocyclic Chemistry 53, 27–33.

Zhang, T.L., Lu, Z.G., Wang, J.Z., Shen, J., Hao, Q.L., Li, Y., J., Y., Niu, Y.W., Xiao, Z.B., Chen, L., Zhang, X., 2021. Preparation of mesoporous silica nanoparticle with tunable pore diameters for encapsulating and slowly releasing eugenol. Chinese Chemical Letters 32, 1755–1758.